Aerothermodynamic Flow Phenomena of the Airframe-Integrated Supersonic Combustion Ramjet

James T. Walton

NOVEMBER 1992

LIBRARY COPY

NASA

NASA Technical Memorandum 4376

Aerothermodynamic Flow Phenomena of the Airframe-Integrated Supersonic Combustion Ramjet

James T. Walton
Lewis Research Center
Cleveland, Ohio

Summary

The purpose of this report is to discuss the unique component flow phenomena of the airframe-integrated supersonic combustion ramjet (scramjet) in a format geared towards new players in the arena of hypersonic propulsion. After giving an overview of the scramjet aerothermodynamic cycle, this report then continues to cover individually the characteristics of the vehicle forebody, inlet, combustor, and vehicle afterbody/nozzle. Attention is given to phenomena such as inlet speeding, inlet starting, inlet spillage, fuel injection, thermal choking, and combustor-inlet interaction.

Introduction

After thermodynamic cycle efficiencies are considered, it is clear that efficient hypersonic flight can only be achieved with the hydrogen-burning supersonic combustion ramjet. This conclusion is verified by figure 1, which presents thrust specific impulse versus flight Mach number: over the hypersonic Mach number range, the hydrogen-burning scramjet performed better than hydrogen- and hydrocarbon-burning ramjets, rockets, and turbojets. However, the scramjet performance shown in this figure is theoretical; the transition from design to production is marked by problems of complex flow patterns within each interacting component. Moreover, it is difficult to understand these flow phenomena and resolve these problems because opinions vary as to the definitions of the terms used to describe the various components. For these reasons and because of the renewed interest in single-stage-to-orbit vehicles, the following sections will review the scramjet aerothermodynamic cycle and then discuss the characteristics of each component using current terminology.

Symbols

A	area
c_p	constant pressure specific heat
M	Mach number
MW	molecular weight
Q	dynamic pressure
Q_r	ratio of dynamic pressures
R	gas constant

s	entropy
T	temperature
γ	ratio of specific heats
ϕ	fuel equivalence ratio

Subscripts:

inj	combustor fuel injection plane
jet	injected flow property
main	capture flow property
t	stagnation condition
0	free-stream station
1	cowl leading edge plane
2	minimum area station
*	sonic condition

Scramjet Propulsion Cycle Overview

The concept for the airframe-integrated scramjet was proposed in the late 1960's and early 1970's after podded engine testing revealed prohibitively high external drag (refs. 1 to 4). This finding was verified by the Hypersonic Research Engine Project (ref. 5) which tested a podded scramjet engine in a free-jet wind tunnel with a mounting similar to that of the SR-71 (fig. 2). A spike inlet was used to efficiently compress the flow and to provide a uniform combustor entrance flow field. The results showed high internal performance, thus validating the cycle feasibility and efficiency, but showed poor installed thrust due to external drag. To minimize the installation effects, the airframe-integrated scramjet was designed to be a flying engine, or a slice of the original podded engine (ref. 6). In other words, the vehicle forebody replaced the podded engine's spike inlet and the vehicle aftbody replaced the plug nozzle (fig. 3).

For this design, at supersonic flight Mach numbers, the vehicle forebody generates a bow shock which decelerates, turns, and vertically compresses the approaching free-stream flow. Flow moving parallel to the forebody is ingested into the internal portion of the scramjet at the cowl leading edge plane. The internal portion of the scramjet is divided into modules to facilitate easier wind-tunnel testing. The inlet to the module can have internal compression from the sidewalls
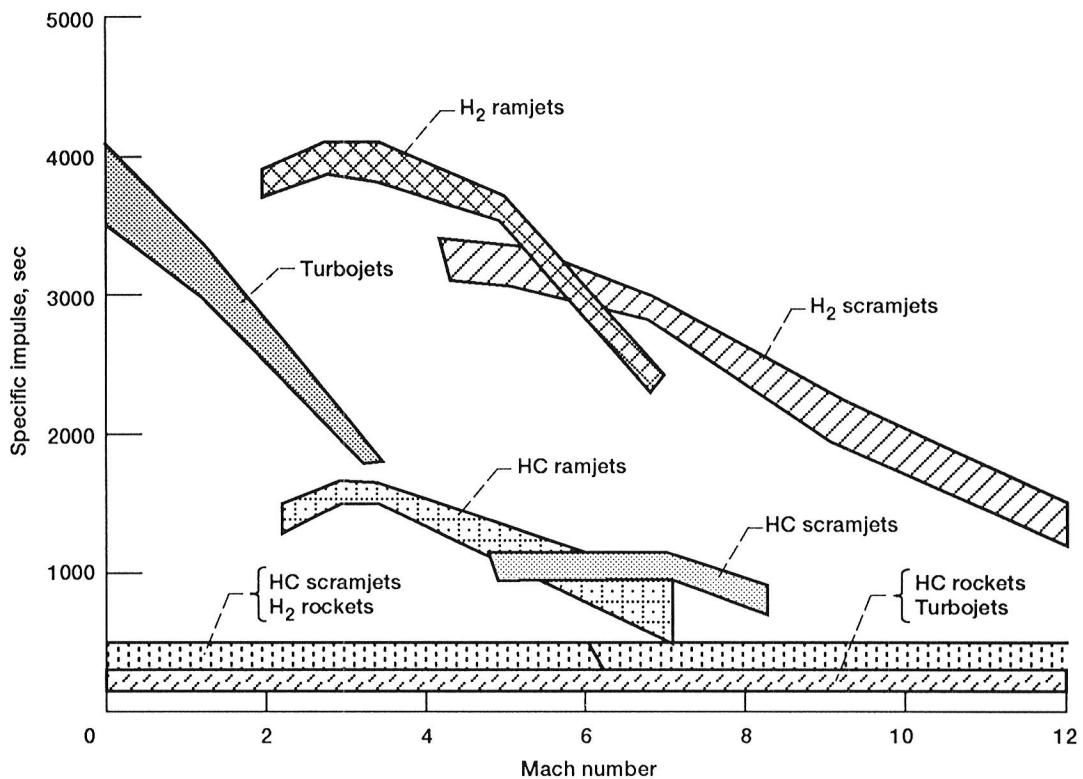
1

Figure 1.—Hydrogen-burning (H_2) and hydrocarbon-burning (HC) propulsion system performances.
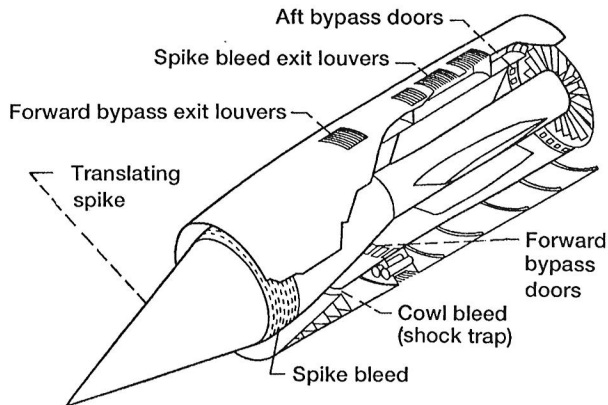

Figure 2.—SR-71 podded annular engine structure.

Figure 3.—Conceptual airframe-integrated scramjet vehicle.

or from the body and cowl walls; these surfaces generate shock waves which compress and slow the flow further. After compression and deceleration, hydrogen is injected into the supersonic flow field. Rapid fuel mixing can be achieved by injecting perpendicular to the flow; however, this results in significant flow disturbance and produces a shock system upstream of the fuel injection. As the fuel is carried downstream, mixing and reaction occur. The mixing rate is a function of flow turbulence whereas the reaction rate is dependent on static pressure and temperature, velocity, and their gradients. The typical residence time of a fluid element
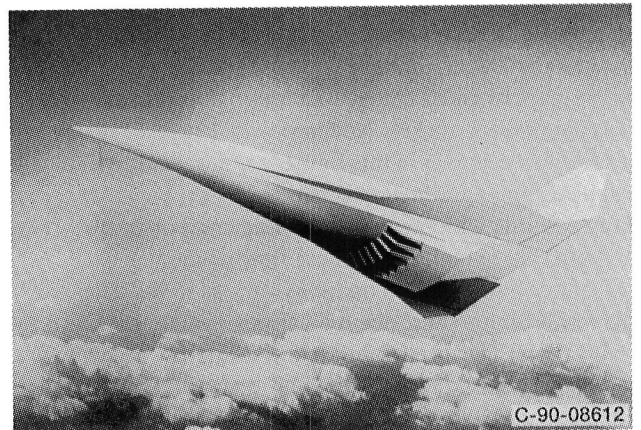
in the module is on the order of 1 msec. After combustion, the flow is expanded internally by diverging sidewalls or body and cowl surfaces and then externally between the diverging vehicle aftbody and exhaust-free-stream shear layer. At high flight stagnation enthalpies, the large heat capacity of the hydrogen fuel can be used to cool the aftbody, as well as the engine module and forebody, by regeneratively circulating the fuel through the structure prior to injection. The scramjet is truly integrated into the vehicle because the forebody provides substantial flow compression while the aftbody provides a bulk of the exhaust expansion to produce thrust.

Scramjet Component Discussion

Vehicle Forebody

As the replacement of the spiked inlet, the vehicle forebody's purpose is to provide precompressed flow to the engine module inlet, which is relatively free of flow gradients; this precompression must be accomplished with minimum drag, heat transfer, and flow stagnation pressure losses (ref. 7).

Inlet speeding.—Precompression is achieved from the shock waves generated by the forebody surface. Since energy has been expended to propel the vehicle supersonically to generate the shocks which compress the flow, it is most efficient to capture all the compressed flow. Total capture occurs when the forebody leading edge shock strikes the cowl leading edge (fig. 4), a condition known as shock-on-lip. At the shock-on-lip condition, all precompressed flow enters the module inlet. From oblique shock theory (refs. 8 and 9), the shock angle for a constant forebody wedge angle increases with decreasing Mach number. Thus, for a lower Mach number, given the same geometry and vehicle angle of attack, the shock wave would pass outside the cowl lip; this condition is referred to as an undersped inlet. Conversely, if the Mach number is greater, the shock falls inside the inlet, a condition known as the oversped inlet. The undersped inlet is less efficient because precompressed flow is turned past the inlet and the spilled high-energy flow is wasted. The oversped inlet is not advantageous since nonprecompressed flow will be entering the module inlet and large flow gradients will exist. The shock-on-lip design point permits maximum flow capture and energy efficiency with minimum flow gradients. However, the shock-on-lip design results in high cowl-lip heat transfer rates from shock impingement.

Flow gradients.—A purpose of the forebody, as part of the integrated system, is to minimize flow gradients (ref. 10). It is desirable to avoid uneven pressure and temperature gradients so that complicated loading and heating patterns in the engine are avoided for design and analysis considerations. Also, uneven mass flow gradients should be avoided so that unique flow fueling schemes need not be designed to create even fuel-air distributions. As mentioned in the Inlet speeding section, major flow gradients can occur when over speeding the inlet.

In addition, other flow gradients exist in the vertical direction across the inlet entrance, in the horizontal plane underneath the vehicle, and in the natural boundary layer entering the inlet off the forebody.

The vertical gradients result from compression waves that come off the vehicle forebody (as shown in the side view of fig. 5) and cause small incremental pressure increases from the bow shock to the boundary layer. The horizontal gradients represent the spread of the flow away from the centerline of the flight path and result from the shock waves off the blunt, conical body shape (fig. 5). This flow expansion causes decreasing flow density from the centerline to the outer engine modules. Note that the degree of this expansion depends on the vehicle's conical or two-dimensional geometry and on the forebody width (the larger the width, the greater the extent of flow expansion).

The last flow gradient is the natural boundary layer (refs. 11 and 12) which is the largest of the gradients and could possibly consume up to half the inlet height depending on design and flight conditions. The boundary layer consists of thermal and momentum gradients. The thermal gradients depend on the forebody wall temperature relative to the flow enthalpy; hence, the temperature is controllable by the degree of active or radiative forebody cooling. The velocity gradient depends on local Reynolds number and the state of the flow: laminar, transitional, or turbulent. In terms of experimental verification of theory, the hypersonic velocity boundary layer is one of the least well defined aspects of the forebody since the forebody tends to be extremely long, and the velocity gradient thickness does not scale well to laboratory size. The implications of this gradient are that (1) in the flow near the vehicle lower surface, mass flow deficiencies will exist and most likely will have to be accounted for in the flow fueling pattern; and (2) the boundary layer state at the point prior to the module inlet should be generated such that the inlet compression can be maximized without exceeding the boundary layer pressure separation criterion. The forebody boundary layer transition should be prior to the inlet entrance. Therefore the peak in the skin friction coefficient (which is related to the heat transfer rate) is encountered before regions of high flow temperature, as in the combustor; this minimizes the overall heat transfer (refs. 11 and 13).
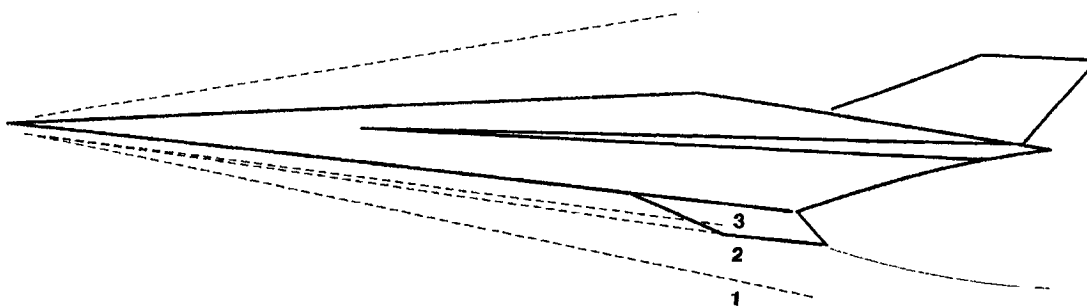

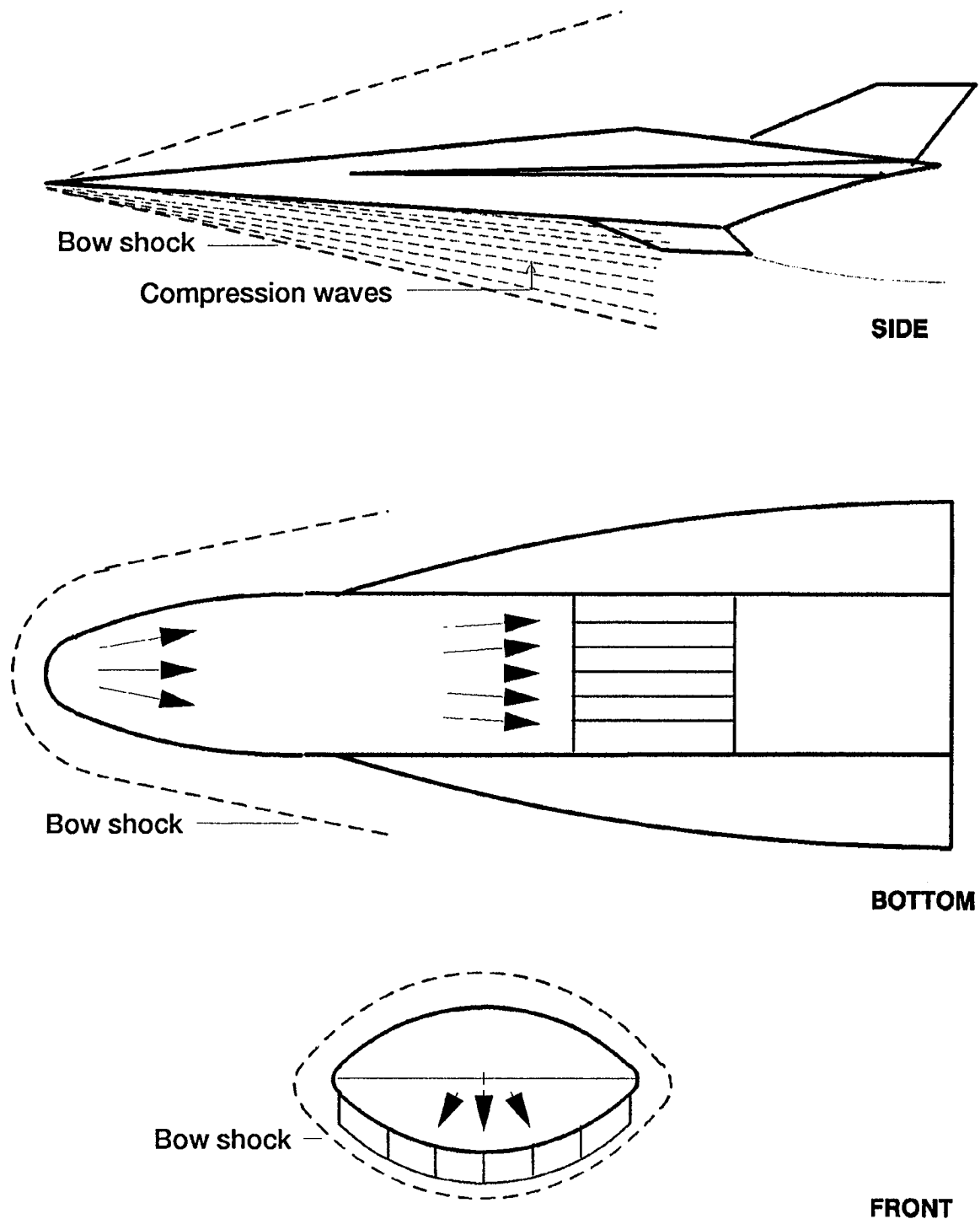Figure 4.—Vehicle inlet speeding (1, undersped; 2, shock-on-lip; 3, oversped).

Bow shock

Compression waves

SIDE

Bow shock

BOTTOM

Bow shock

FRONT

Figure 5.—Vehicle forebody flow gradients.

Multiple forebody wedges.—To minimize stagnation pressure losses during the forebody shock wave precompression process, the forebody should be constructed with multiple wedges. It is more efficient to turn the flow to the same net angle with several wedges, thus minimizing the strength of any individual shock (ref. 8, pp. 336–339). Figure 6 illustrates

this minimization method with only two forebody wedges for various Mach numbers. Since the multiple-wedge concept could result in complex inlet entrance conditions, all possible Mach number regions and subsequent shock angles must be examined. This multiple-wedge concept can be extended to the limit when a smoothly contoured forebody yields a nearly
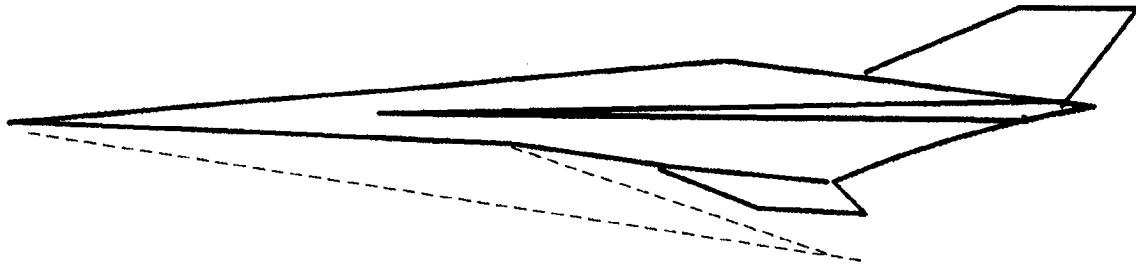
Low Mach Number
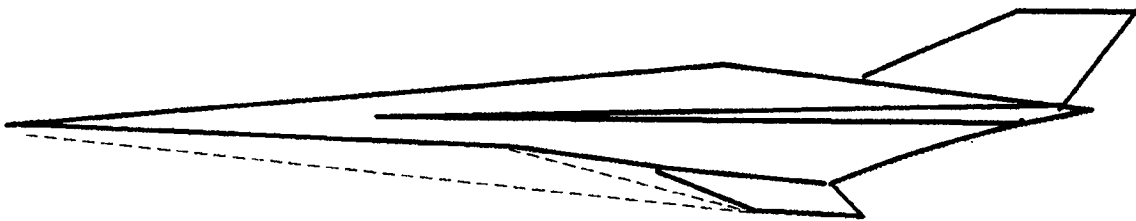
Mid Mach Number
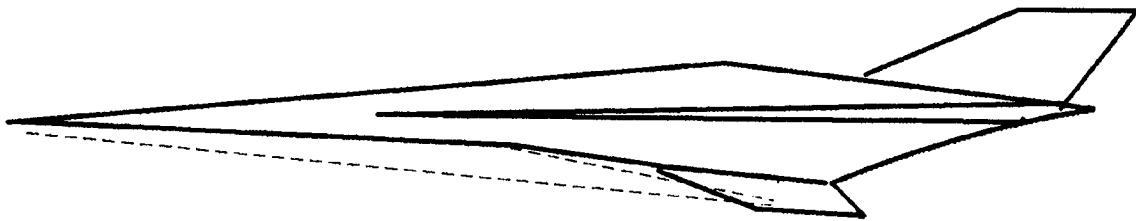
High Mach Number

Figure 6.—Dual-forebody wedge shock patterns.

isentropic flow from the free stream to the inlet entrance. The precompression is completed by Prandtl-Meyer waves (ref. 8) and results in essentially no inviscid stagnation pressure losses and no complex inlet flows. However, the forebody surface is difficult to manufacture on a large scale and could be unfeasible. Moreover, the precise contour is Mach number dependent.

Angle of Attack.—Since there is such a close margin between engine thrust and drag, as demonstrated by the annular podded engine tests, it is important to optimize all forebody parameters in relation to the internal module and vehicle afterbody (ref. 14). The forebody can contribute a substantial portion of the compression (about 30 percent) for thrust (ref. 6). The amount of precompression the forebody provides to the flow entering the scramjet module is a function of the wedge angle(s) relative to the flight direction. Therefore, the vehicle angle of attack plays an important role in the forebody, as well as in the overall system performance (ref. 15). This fact is

illustrated in figures 7 and 8 for a generic airframe-integrated scramjet vehicle from two-dimensional computational analysis.

Engine Module Inlet

With regard to the airframe-integrated scramjet, the module inlet is usually defined as beginning at the sidewall leading edges and ending at the minimum area station. Because some

designs require a long constant minimum area section to isolate the combustor from the inlet, the inlet is considered to end at the start of the constant area section. If the inlet were to begin at the sidewall leading edges (if this station is ahead of the cowl leading edge), inlet shocks may cause some flow spillage.

The purpose of the internal inlet is to provide main compression to the captured flow by using geometric contraction
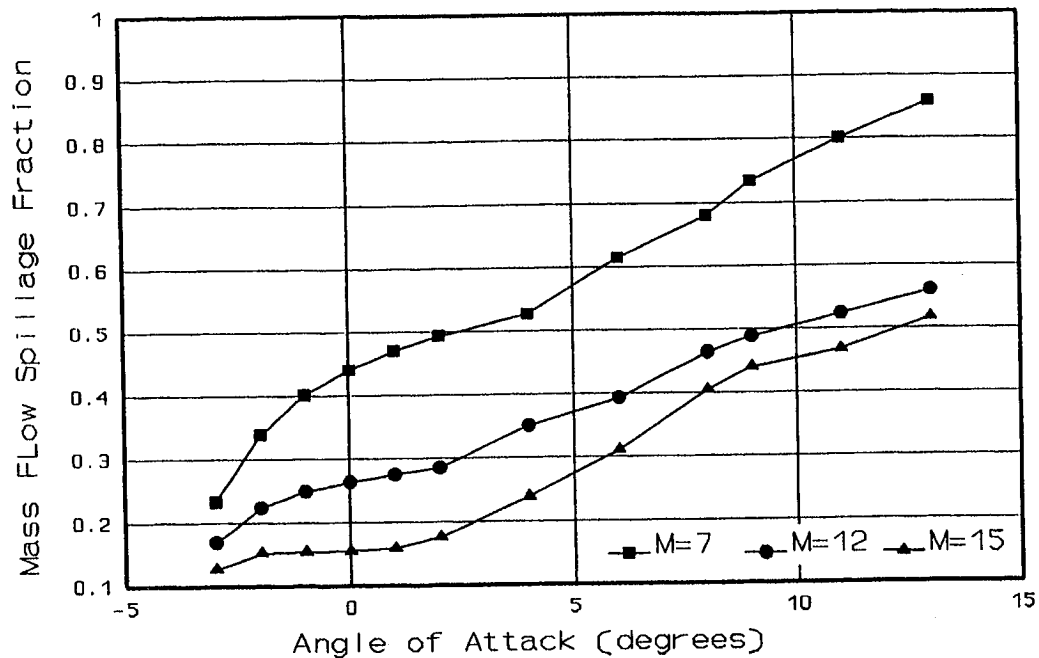
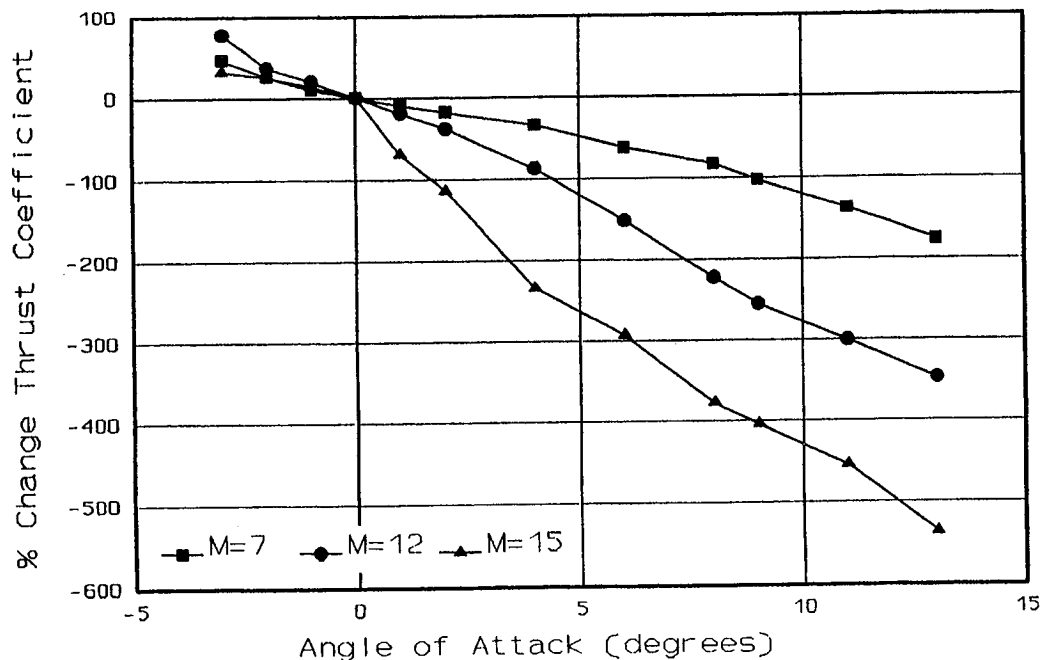Figure 7.—Spillage as a function of angle of attack for a generic vehicle.

Figure 8.—Thrust as a function of angle of attack for a generic vehicle.

and shock waves. Typically, inlet designs call for shocks originating on the sidewalls or on the body and cowl. Other inlet functions include preventing boundary layer separation, providing uniform combustor flow and allowing high contraction but good starting capability. The inlet should be designed for low heat transfer, drag, and stagnation pressure losses (ref. 16).

Inlet starting.—At flight Mach numbers less than 5, high internal contraction is a tradeoff against the ability to pass a supersonic flow through the inlet (i.e., start) for fixed geometries. High contraction implies a large entrance area to capture as much of the forebody flow as possible; it also implies high compression to pass high pressure flow into the combustor for improved performance. In this Mach number range, a maximum aerodynamic contraction ratio exists for an inlet to start. The aerodynamic contraction differs from the physical contraction by the amount of inlet spillage (from a cutback cowl design) and by boundary layer momentum thickness. Therefore, for a fixed geometry, inlet starting may necessitate that spillage be increased to reduce the aerodynamic contraction (ref. 17); spillage is achieved by either dumping flow out of the inlet through porous surfaces (bleed) or by turning the approaching flow downward by shock waves generated from the swept-sidewall leading edges (fig. 9). The usage of inlet sidewall sweep to turn the flow down is attractive since, as the Mach number increases, the angle of turning decreases and less flow is spilled; the resulting higher aerodynamic contraction is acceptable based on the inlet starting criterion as the Mach number increases. Inlet sidewall sweep angles tend to be between 30° to 60° from the vertical.

The general inlet starting criterion which yields the maximum aerodynamic contraction ratio for an isentropic perfect gas is (as developed by Kantrowitz (ref. 18))

$$\text{Percent spillage} = \frac{\text{Projected capture flow}}{\text{Projected flow}}$$
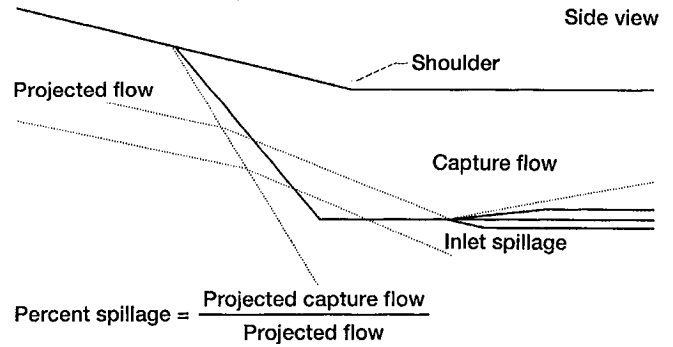
Figure 9.—Inlet spillage flow diagram.

distributions for the engine module section of an airframe-integrated scramjet when contraction is increased. For this configuration, inlet contraction was increased by rotating the cowl away from the body because there was no sidewall compression. At a geometric area ratio of 1.35, the inlet unstarted. The Kantrowitz criterion predicts that this inlet will start at an aerodynamic contraction of 1.27.

Combustor-inlet interaction.—The inlet can also be unstarted by increasing the back pressure from the combustor. Increasing fuel flow rates or reducing the nozzle area results in an increase in combustor pressure. As combustor pressure rises to a critical level, the inlet throat boundary layer separates and combustor-inlet interaction occurs (refs. 20 and 21). The separated region reduces the flow area in the inlet throat, which can choke the flow and produce an unstart. In other words, the increased combustion or nozzle area reduction can overchoke the flow, which can change upstream conditions and lead to an unstart. Figure 11 illustrates the effects on the inlet of increasing the combustor pressure level. As the combustor pressure

$$\frac{A_1}{A_2} = \frac{[(\gamma + 1)/(2\gamma M_1^2 - \gamma + 1)]^{1/\gamma - 1}\{(\gamma + 1)M_1^2 / [(\gamma - 1)M_1^2 + 2]\}^{\gamma/\gamma - 1}[1 + (\gamma - 1)M_1^2/2]^{(\gamma + 1)/[2(\gamma - 1)]}}{M_1[1 + (\gamma - 1)/2]^{(\gamma + 1)/[2(\gamma - 1)]}}$$

From the equation, with a peak value of 1.5 around Mach 5, the benefits of variable inlet contraction as opposed to fixed geometry are clear. Note that the criterion computes the maximum aerodynamic contraction ratio; therefore, this value is always greater than the geometric contraction after the boundary layer and separated regions are taken into account (ref. 17). More detailed inlet starting criteria are discussed in reference 19.

Inlet unstarting.—Once an inlet is started with supersonic flow throughout, using the general starting criterion, contraction can be further increased until the flow Mach number at the minimum aerodynamic area station is driven sonic. A further increase in contraction will unstart the module's inlet. Inlet unstart is undesirable because it generates high pressure levels and because the terminal shock system ahead of the unstarted module can affect an adjacent module. Figure 10 shows the axial body and cowl wall static pressure

increases, the effects are seen farther and farther upstream until they enter the constant-area section (combustor-inlet interaction). As the combustor pressure is further increased, the inlet unstarts. Note that, as flight Mach number increases, the potential for inlet unstart due to back pressure decreases; this decrease occurs because the combustion enthalpy is less relative to the capture flow total enthalpy. Generally, a back-pressure unstart is not likely above Mach 8.

As shown by the previous pressure distributions, the unstarted data exhibited a large gradual pressure rise commencing ahead of the cowl leading edge and extending downstream into the constant-area section. Unstarts for configurations like this are not manifested by a normal shock standing in front of the cowl but by a strong oblique shock beginning on the ramp at a boundary layer separation point ahead of the cowl leading edge plane. Under high inlet back-
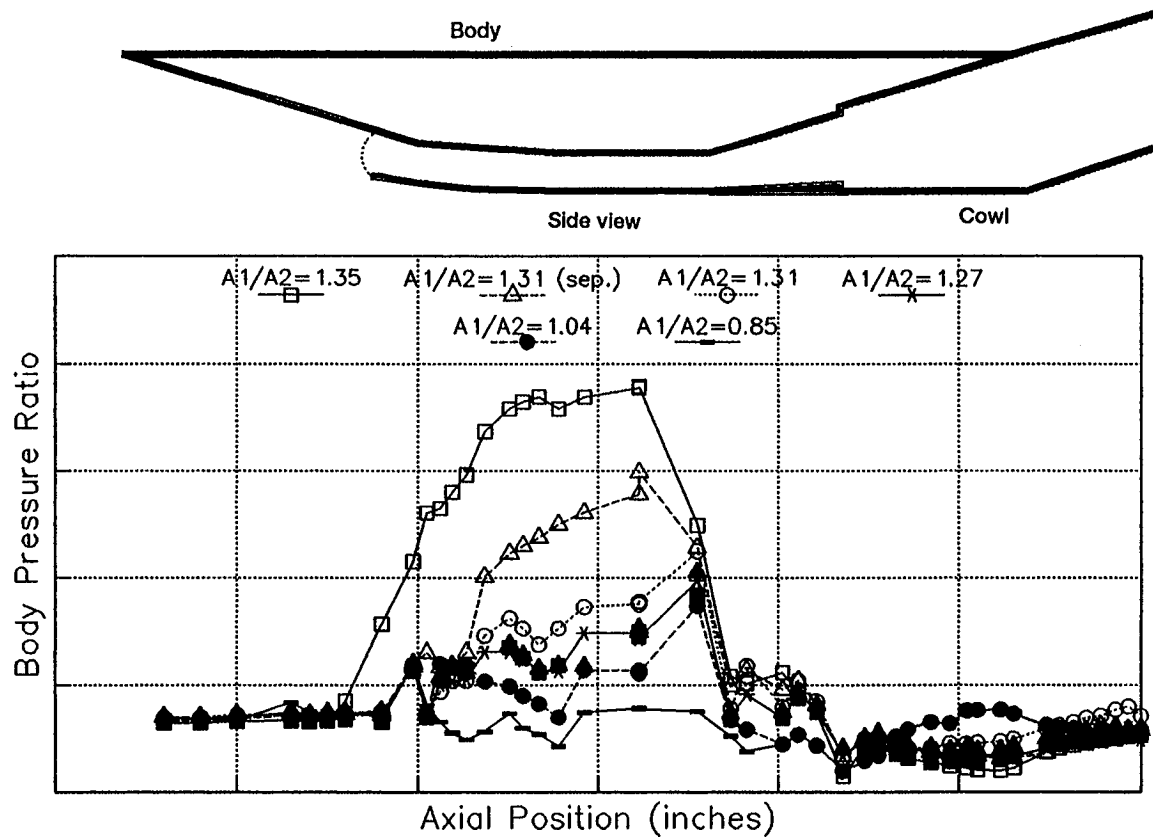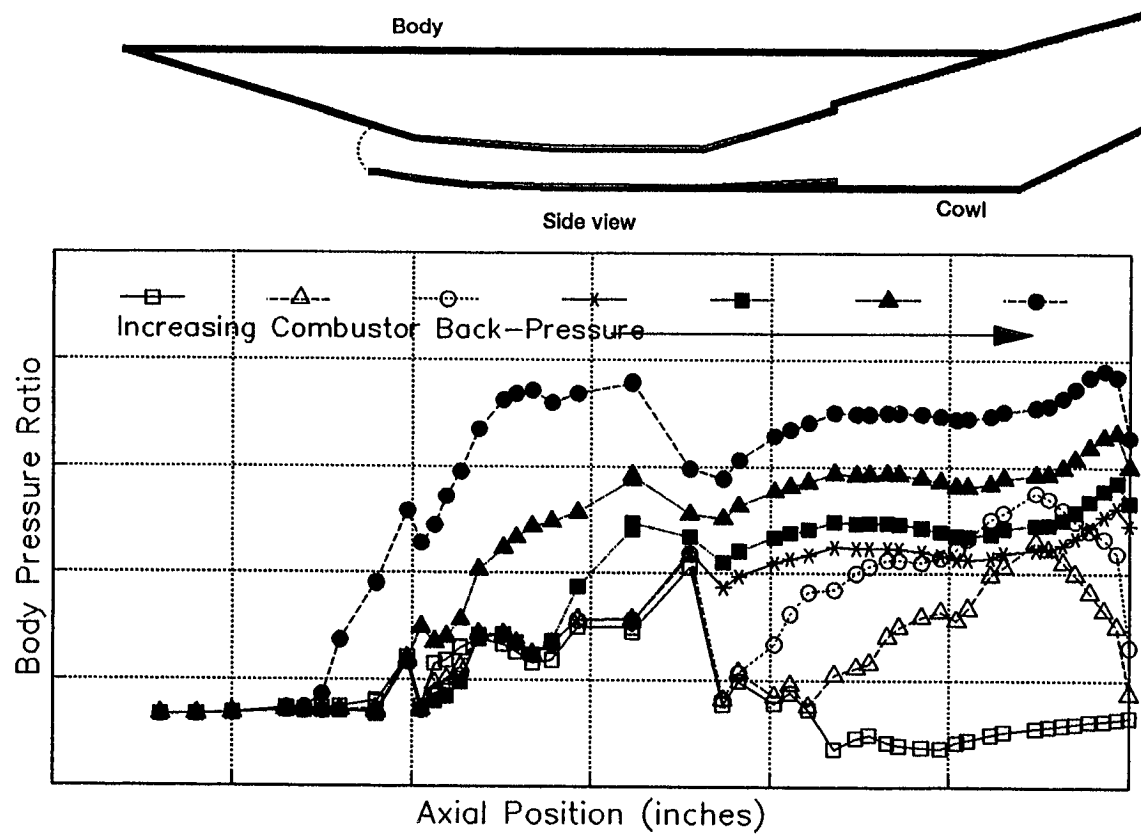
(a) Body wall static pressure distributions.
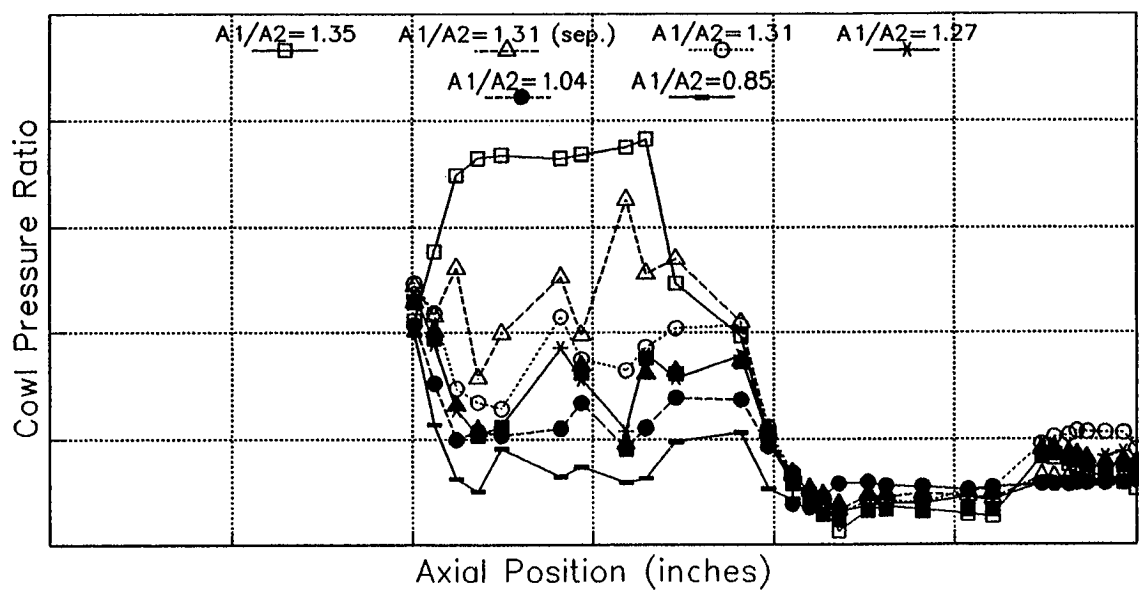
(b) Cowl wall static pressure distributions.

Figure 10.—Effects of increasing inlet contraction ratio on static pressure.

Body

Side view   Cowl

Increasing Combustor Back—Pressure ————————▶

Body Pressure Ratio

Axial Position (inches)

(a) Body wall static pressure distributions.

Cowl Pressure Ratio

Axial Position (inches)
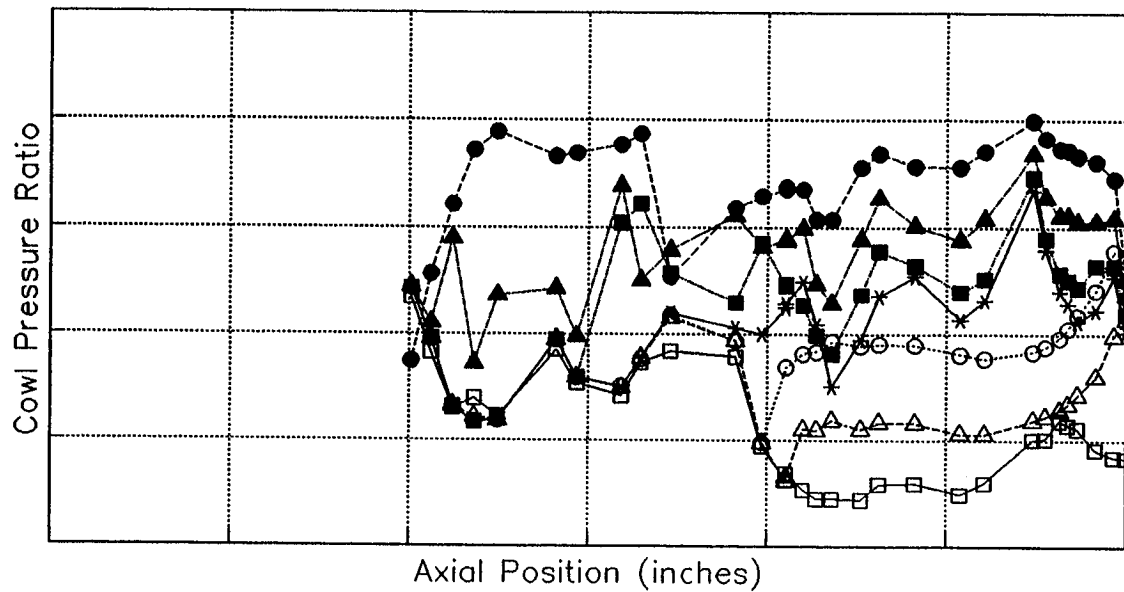
(b) Cowl wall static pressure distributions.

Figure 11.—Effects of combustor back pressure on the inlet.

pressuring conditions, this terminal shock system can undergo a large amplitude oscillation known as "buzz" (ref. 16, pp. 269–291). The buzz condition should be avoided because of the large amplitude of the pressure oscillations.

Inlet bleed.—As the combustor back-pressure is increased, the onset of combustor-inlet interaction well precedes engine unstart. Because unstart occurs at the maximum combustor pressure level, which is the desirable operating condition, it is advantageous to delay the onset of combustor-inlet interaction (inlet boundary layer separation) to back-pressure levels near those required for unstart. Thus, high inlet performance and uniform exit flow can be maintained. Combustor-inlet interaction can be delayed by changing the boundary layer history upstream of the inlet-combustor interface. As seen in figures 10 and 11, once combustor-inlet interaction occurs, the boundary layer separates up to the inlet shoulder (fig. 9).

For the supercritical inlet (i.e., no back pressure), the shoulder geometry significantly affects the downstream boundary layer history. Inlet designs generally call for the cowl lip shock to be reflected or canceled at the shoulder. The shock-boundary layer interaction at the shoulder tends to generate a small separated region which quickly reattaches, but this affects all downstream boundary layer properties. However, upon high back pressuring, the boundary layer to the minimum-area station can separate up to the shoulder separated region. Since the level of back pressure before incipient separation is a function of upstream boundary layer growth (ref. 22), the maximum back-pressure level can be raised by bleeding off the boundary layer at the shoulder and by controlling the shock-boundary layer interaction. The benefits of flush wall bleed (fig. 12) in delaying combustor-inlet interaction have been evaluated experimentally and the results are discussed in references 22 to 24. The usage of bleed allows delaying the combustor-inlet interaction until unstart. Because bleed reduces boundary layer growth, in a lower aerodynamic contraction results; therefore, a secondary benefit is realized since higher geometric contraction (capture) can be used without unstart (fig. 13). The benefits of bleed on the body
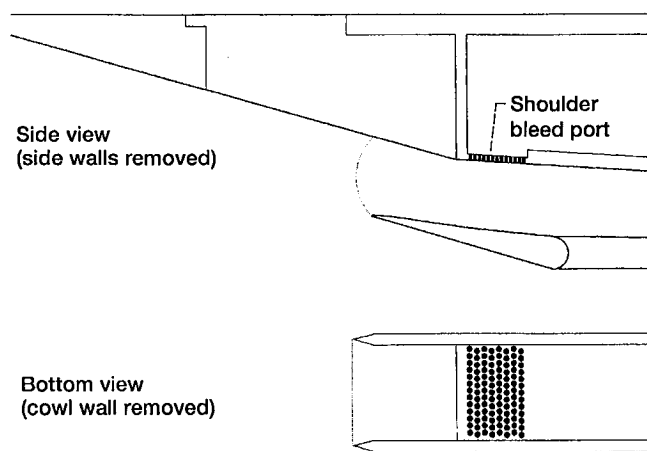
Figure 12.—Inlet shoulder bleed diagram.

surface with regard to the removal of the large forebody boundary layer are shown in figure 13. Note that, because no bleed was used on the cowl, a back-pressure level was reached prior to unstart and the cowl boundary layer was separated. Cowl boundary layer separation up to the leading edge can detach the lip shock and result in flow spillage and reduced mass capture. The main disadvantage of bleed is the problem of disposing of the bleed flow. A related question is whether or not the increased combustor performance offered by bleed is greater than the bleed drag penalty. Moreover, designing a bleed system to handle high enthalpies is a problem unless a closable, flush-slot bleed system is used.

Inlet aspect ratio.—Ideally, like the podded axisymmetric engines, the airframe-integrated scramjet vehicles would have an engine module which wraps around the entire vehicle circumference. However, this design was not feasible because of the wing and landing gear placement and the large engine size. For convenience, the large engine module was wrapped around only the vehicle lower surface and was divided into equal segments, each approximating a rectangle. Thus, the many smaller modules, which can be more easily tested, were combined on the vehicle undersurface as the propulsion system. The rectangular inlet is a balance between height and width; the quotient of these is the aspect ratio. Taller inlets tend to be more difficult to start because it is harder to get the flow to spill down vertically over the larger height. However, taller inlets allow a greater capture of the approaching mass flow. A tall inlet with good starting will be longer and thus have higher drag and heating loads. The inlet width is limited by the combustor; fuel is conveniently injected from the sidewalls and, therefore, width is limited by the extent of penetration. The balance between height and width is shown by the several inlet configurations (ref. 25) in figure 14.

Even with a careful balance, fuel penetration can still be a problem. Figure 15 shows the concept of a "first-generation" airframe-integrated scramjet engine with a sidewall removed (ref. 26). In this configuration, three struts are utilized to turn the flow down to spill at low Mach numbers and to provide substantial compression due to shocks and geometrical contraction. With the struts, contraction can occur rapidly in a short length and with low turning angles (6 deg). Also, the latter half of the struts provides a surface from which to inject fuel, with a small gap for good penetration. However, with fuel injection and reaction so closely coupled to the inlet compression, an undesirable combustor-inlet interaction can occur. Moreover, it is not reasonable to have any protrusion into the flow at high flight Mach numbers because of the high stagnation temperature.

Combustor

The term scramjet implies that the Mach number of the flow at the fuel injection station is at least supersonic prior to fuel injection. This definition was chosen because either of two
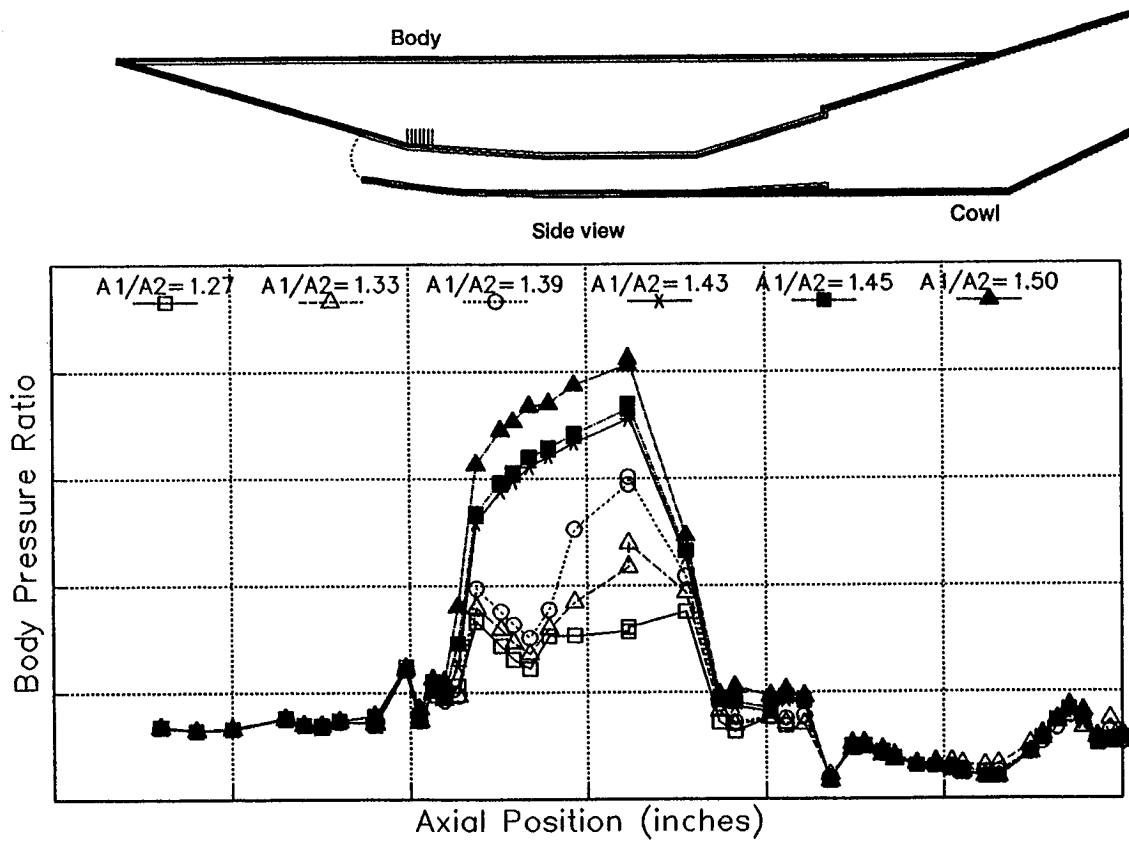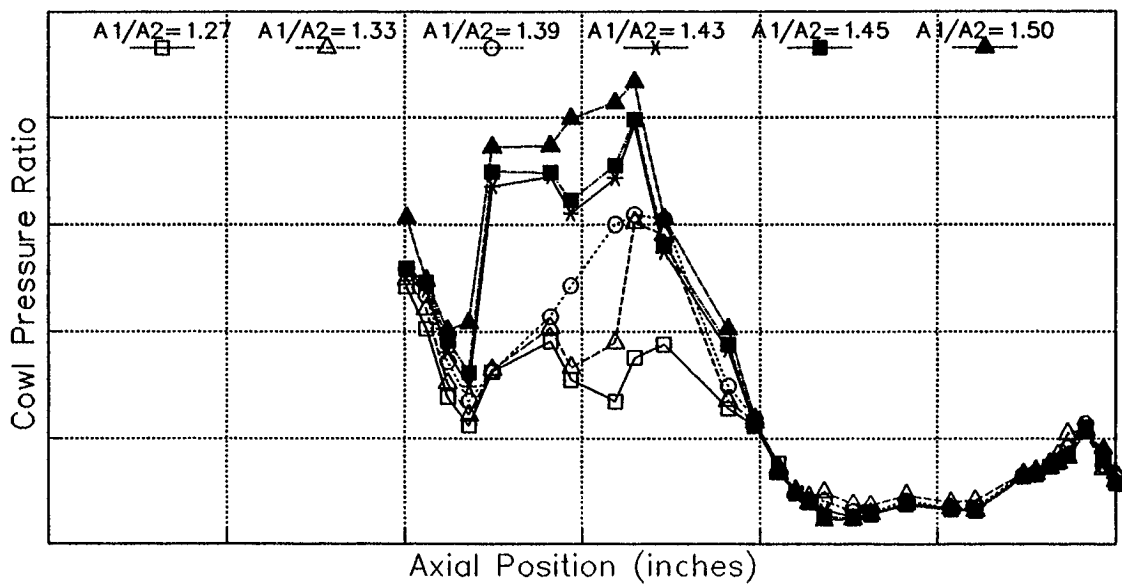
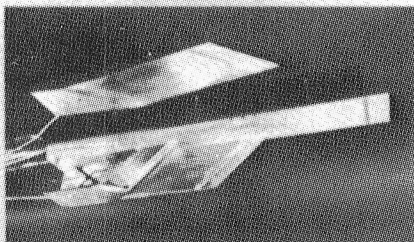(a) Body wall static pressure distributions.
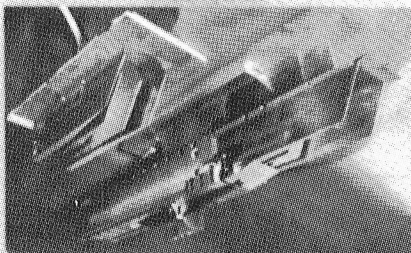

(b) Cowl wall static pressure distributions.

Figure 13.—Effects of increasing inlet contraction ratio for configuration with 5 percent bleed flow.

HYPERSONIC INLET DESIGN

INLET MODELS
Three-strut

Two-strut

No strut

Step strut
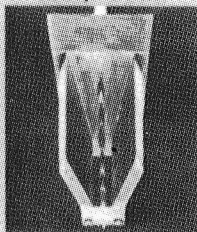
Inlet Research

- Existing
  - Experimental data base for swept, rectangular sidewall, compression inlets
- Planned
  - Performance for Mach 3.5 to 18
  - Inlet starting
  - Combustor/inlet interaction
  - Code validation for Mach 3.5 to 18 in air and helium
  - Highly cooled wall effects on inlet performance

CFD FLOWFIELD
Two-strut inlet

INLET MODELS
Reverse sweep
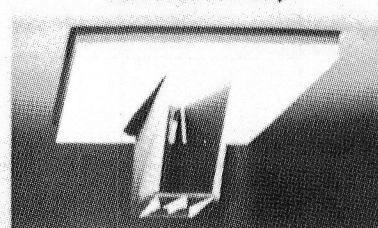
Three-module
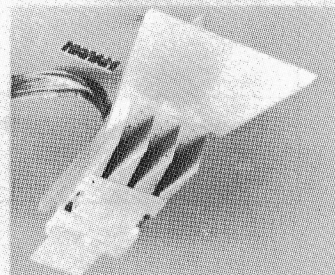
Rectangular to circular
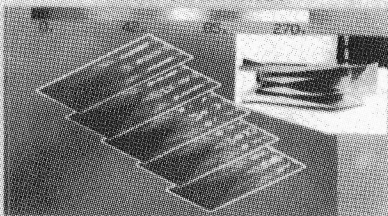
C-90-08611

Figure 14.—Various fixed geometry inlets.

Figure 15.—Three-strut engine concept.

processes may choke the flow: the fuel injection, with related shocks and separations, or the combustion. Thus, a scramjet may contain some regions of subsonic flow. The purpose of the combustor is to maximize the rates of fuel mixing and reaction, within combustor-inlet interaction and unstart limits, while minimizing total pressure losses and combustor surface area.

Currently, the only realistic choice of fuel for a single-stage-to-orbit mission is hydrogen (ref. 27), which is stored in cryogenic tanks as either a liquid or a partial solid (slushed). Hydr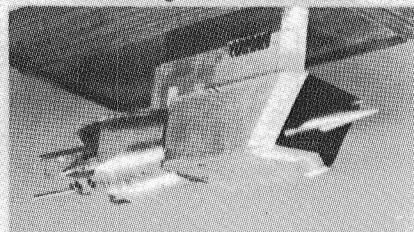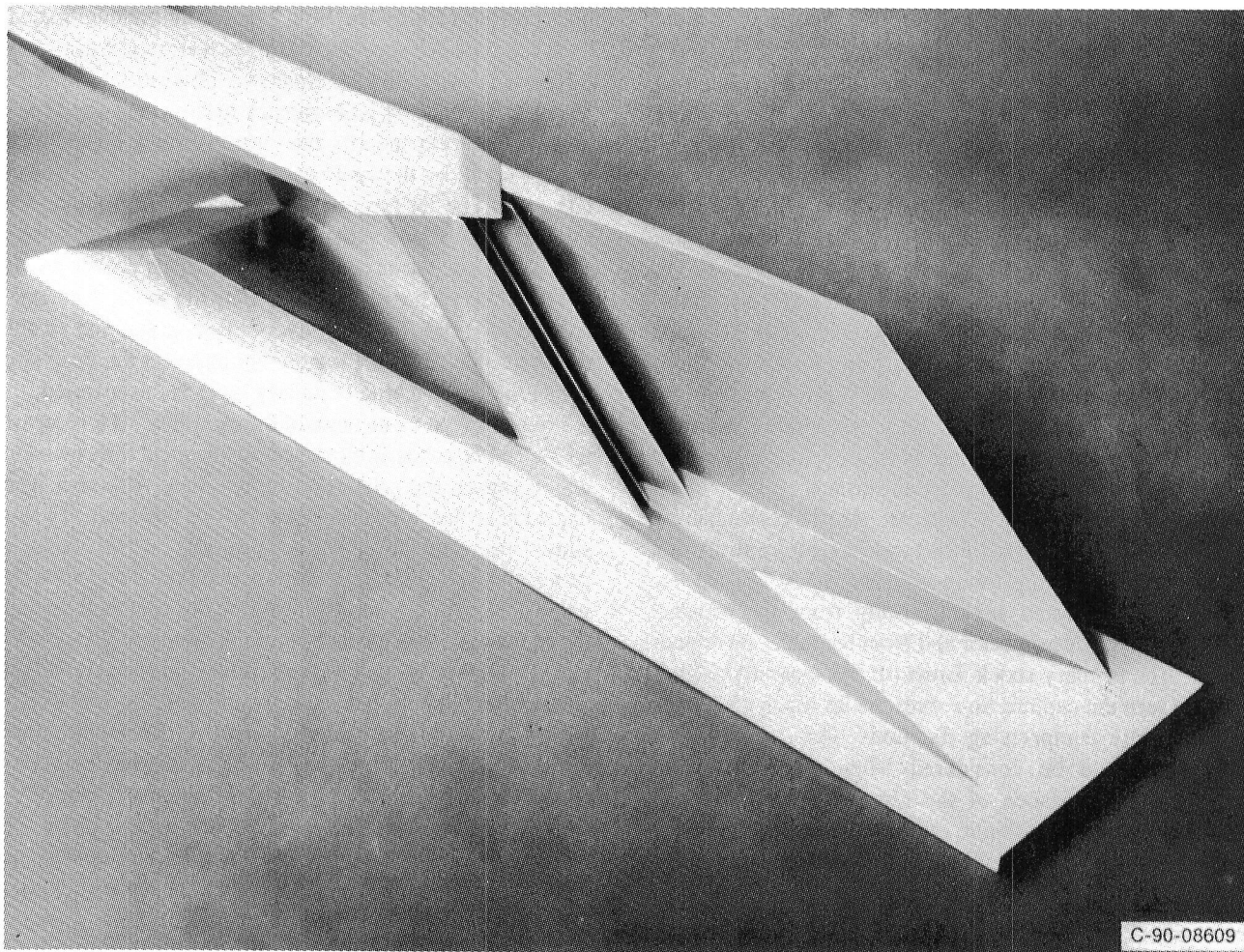ogen is advantageous because of its heat capacity, which can be used for structure cooling, and its high flame speed, but it is disadvantageous because of its low density. For hypersonic cruise vehicles, hydrogen-hydrocarbon fuel blends, such as the use of ethylene, have been considered (ref. 28) to improve the stored fuel density; however, the lower flame speeds necessitate longer combustors.

Injection process.—Traditionally, combustors have been designed for gaseous fuel injection either parallel or perpendicular to the capture flow, although angles between have been considered. The combustor sidewalls are convenient injection locations; however, in some designs, injection was from the body or cowl surfaces or from vertical fuel injection struts within the flow. A large diverging surface is a poor injection location because the pressure rise from the injection and combustion processes in most cases separates the boundary layer upstream to the beginning of the diverging surface.

Parallel injection is advantageous because it allows all the fuel momentum to contribute to axial thrust; however, since fuel mixing and spreading are caused by the interacting shear layers, long combustors are required for complete mixing. Another advantage is that parallel injection along a planar combustor wall reduces the heat load on the wall (generally known as film cooling). Perpendicular injection allows for deep fuel penetration and rapid mixing; however, it creates a large flow disturbance and none of the fuel momentum is recovered as axial thrust.

It is important to recognize that the combustor wall boundary layer is already close to the incipient turbulent boundary layer separation limit (ref. 29) because of the large forebody boundary layer entering the inlet and the rapid rise in inlet pressure. At flight Mach numbers where perpendicular fuel

injection is advantageous, the fuel injection process is a source of boundary layer separation. As shown in figure 16, sonic perpendicular fuel injection from the sidewall produces a unique flow field about the fuel jet. The main structures in this flow field are (1) the jet expansion fan and barrel shock, (2) the upstream and downstream separated boundary layer regions with recirculation, and (3) the bow shocks off the separation and reattachment regions. The height of the barrel shock (Mach disk) is usually the extent of the mean fuel penetration whereas the expansion fan edges are the limits. The bow shocks are significant because their strength tends to increase with the fuel equivalence ratio ϕ. At low flight Mach numbers, these shocks are disadvantageous because the increasing shock strength lowers the Mach number at which combustion occurs; Mach number is a controlling parameter on the maximum value of ϕ prior to unstart.

Aerodynamic contraction.—With regard to the perpendicular fuel injection flow field, one of the most interesting structures is the separated region upstream and downstream of the jet. The upstream separated region results from the adverse pressure gradient at the injector and from boundary layer path blockage. The primary shock forms off the separated region in order to turn the capture flow over the jet Mach disk, thus aerodynamically compressing the flow. This aerodynamic contraction should be considered when evaluating inlet starting. The significance of the separated region is that recirculation can occur within it, often entraining fuel. Because of the long residence time in this region, combustion can occur and further increase the separated region size. Thus, depending on the injectant mass flow rate and ratio of jet to capture flow dynamic pressure Q_r, recirculation can occur and cascade to full surface boundary layer separation. Since heat release in the recirculation region is known to contribute to the adverse pressure gradient as the flight Mach number increases, the relative effect of combustion enthalpy decreases and separation lessens. It is important to note that separation on one surface affects the boundary layer on other surfaces.

Penetration.—As noted in the previous section, the limit to fuel penetration for perpendicular injection is the height from the surface to the Mach disk. For the fuel to penetrate the flow, the fuel stagnation pressure must exceed the surface static pressure. The extent of fuel penetration is a function of the ratio of jet to capture flow dynamic pressure (ref. 6). The following equation can be used to compute the dynamic pressure ratio Q_r:

$$Q_r = 0.02916\phi(A_{\text{main}}/A_{\text{jet}}M_{\text{main}}/M_{\text{jet}})$$

$$\times \left[\gamma_{\text{jet}}MW_{\text{main}}T_{t\text{jet}}/(\gamma_{\text{main}}MW_{\text{jet}}T_{t\text{main}})\right]^{0.5}$$

Typically, the penetration height is a function of Q_r raised to the power in the range of 0.25 to 0.5.

From an analytical view, the emergent jet can be considered a solid body emerging from the port and subsequently being bent downstream by the flow particle momentum exchange. The solid body's cross section is distorted by a pressure differential from the upstream to downstream surface by viscous shear and by jet expansion to flow pressure. Since the jet is underexpanded, the turning and distortion are accompanied by the rapid area expansion and normal shock (fig. 16). The jet turning is elliptical (refs. 30 and 31).

The primary bow shock in the main flow is caused by the obstruction of the primary flow by the emergent jet. If the pressure rise on the surface caused by the shock is greater than about 3 to 1, the boundary layer will separate, and an oblique shock off the separated region will intersect the main stream. When the approaching boundary layer is unseparated, the jet is exposed to the momentum of the main flow. If it is separated, the jet will be partially blocked from the main flow momentum, depending on the separation region size. Although it might appear that this would increase fuel penetration, it has been shown that separation region size only slightly affects the penetration height. The reason is that, for a constant Q_r and mass flow rate, few parameters actually change the height of the Mach disk, and the momentum losses across the disk limit the penetration of gaseous jets into a supersonic stream. It seems, then, that the advantage would be to have a large initial jet momentum, such as that with a supersonic injector. However, for equal mass flow rates, this has resulted in a maximum 25 percent increase in penetration (ref. 32). In short, the high momentum of the supersonic airstream causes the injected fuel to be turned rapidly downstream, limiting mixing and combustion efficiency, especially if opposite wall injectors fail to fuel at least half the gap between them.

Mixing.—As mentioned in the section Injection process, combustor designs require that injection be either parallel or perpendicular to the flow, although angles between have been considered. Generally, decreasing the angle from perpendicular (normal) to parallel (tangential) results in reduced penetration and lower injection-induced shock losses and also increased tangential fuel momentum. Perpendicular injection sacrifices axial fuel momentum (potential thrust) for improved penetration and mixing. When injected perpendicularly, the induced shocks generate turbulence and magnify the flow turbulence which breaks the fuel jet macroscopically into many small eddies. As the angle of injection decreases to parallel, the shear layer between the stream and fuel causes macroscopic mixing. This mixing results from the turbulent eddies which are produced as the shear layer decays.

In both cases, molecular diffusion is responsible for microscopic mixing. The rate of diffusion is high at first because of the large gradients in concentration, pressure, and temperature (from mainstream to jet). Then the rate decreases and levels off downstream (ref. 33). For perpendicular injection, the rate of mixing decays logarithmically whereas for parallel injection it decays semilinearly with axial position, as seen in figure 17.

As with penetration, main flow velocity plays an important role in fuel mixing. Logically, if the main flow velocity is

Side View

Top & Bottom Wall
Boundary Layers

Fuel Injectors

Bottom View

Side Wall
Boundary Layer

Fuel Injectors

Primary Bow Shock

Boundary Layer

Mach Disk

Jet Boundary

Separated

Recirculation

Expansion Region

H_2
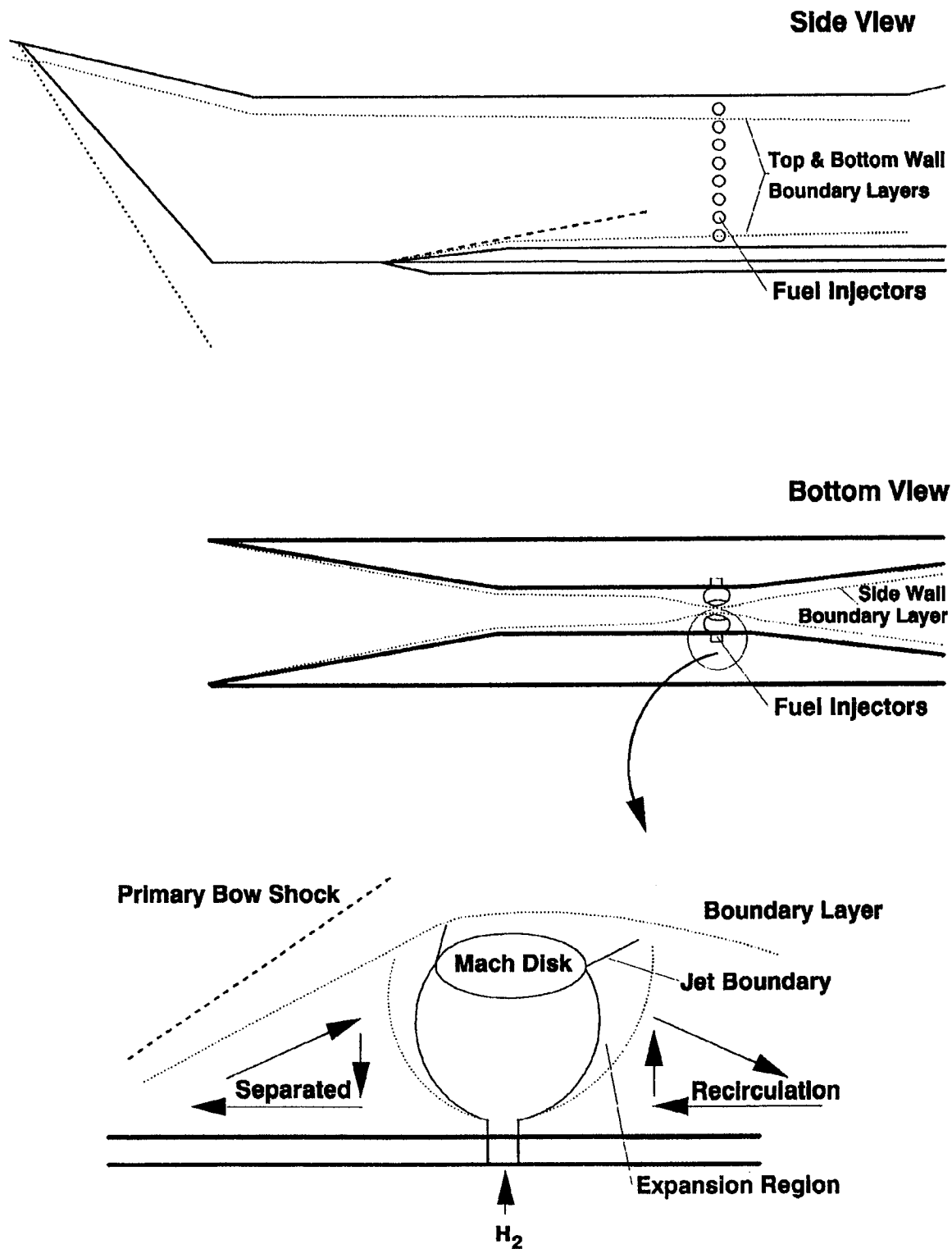
Figure 16.—Fuel injection schematic and flow field nomenclature.

Figure 17.—Typical axial fuel mixing distribution profiles.

The reaction rates for bimolecular reactions (1 to 3) are faster and dominate the initial phase of combustion between new microscopically mixed H_2 and air. In this free radical production phase, no temperature rise occurs. As the radical concentration increases, the other reactions gain in stature; the time delay prior to this is the ignition delay time and is characterized by large concentration changes in H_2O, O, OH, and in an H-radical concentration peak. The ignition delay is a prelude to the recombination of atomic H and O from which most of the reaction enthalpy is released. The time to proceed from the end of the ignition delay to an equilibrium state is the reaction time. This period is characterized by the large temperature changes. In comparison to the reaction time, the ignition delay time is more inversely affected by temperature whereas the reaction time is more inversely affected by pressure. The three-body recombination reactions (6 and 7) explain this pressure influence. The total residence time, the other factor in the reaction efficiency definition, is the combustion length divided by the flow velocity; the value for scramjets is on the order of .1 msec. With respect to structural loads and cooling, short combustors are mandated. Therefore, good overall combustion efficiency depends on a combustor design that ensures good mixing and flow properties that result in short ignition delay and reaction times.

Flame structure.—The combustion flame type is controlled by the reaction rates and is important for combustion efficiency. Two well known flame types are the diffusion flame and the heat conduction flame. A third type not well investigated is the transonic/reverse flow flame (ref. 39).

The diffusion flame is generated when the chemical reaction rates are favorable, the reaction taking place instantaneously upon fuel and air microscopic mixing. Ideally, the properties of the flow entering the combustor are such that the diffusion flame results.

The second type of flame, the heat conduction flame, is generated when the bulk flow temperature is below that of the fuel autoignition temperature. The general reaction is controlled by the conduction of heat from the ignition source through the flow. The point is that even though the flow is homogeneously mixed and reaction rates are high (due to high static pressure), the local temperature can be below the fuel autoignition limit (refs. 36 and 38), hence limiting the combustion efficiency. This flame type is extremely important with respect to attaining supersonic combustion at low flight enthalpies. When ignition sources and flow stagnation points are excluded, the wall boundary layer provides a special ignition region for this flame. At hypersonic velocities, the static temperature in the boundary layer is much higher than in the free stream, especially if the wall temperature is higher than free stream. Hence, fuel and air mixed in this region react rapidly and provide an important source for ignition and heat conduction. From a consideration of this flame type and in an attempt to attain supersonic combustion at low flight Mach numbers, it appears desirable to have a low Mach number at the combustor entrance, thus increasing the static

decreased, an incremental volume of fuel and air will have a longer residence time together in the combustor, hence yielding increased mixing at a given combustor station. This situation occurs when aerodynamic blockage results from fuel injection. As the fuel equivalence ratio increases, flow velocity decreases slightly, leading to improved mixing. Because the residence time is increased, a higher percentage of the fuel and air is microscopically mixed, thus leading to an increase in combustion efficiency (ref. 34).

Reaction.—Combustion efficiency is defined as the product of mixing efficiency and reaction efficiency. Mixing efficiency is the quotient of the area-integrated local fuel equivalence ratio divided by the injected equivalence ratio; reaction efficiency is the quotient of the reacted fuel-air mass divided by the total fuel-air mass that can react. If the reaction rates are fast with respect to the mixing rate, then the flow combustion efficiency will be approximately equal to the mixing efficiency and a diffusion flame will result. On the contrary, if the reaction rates are slow relative to the mixing rates, then the combustion efficiency will be equal to the reaction efficiency, and a heat conduction flame will result because further ignition is dependent on heat conduction from the ignition source (refs. 35 to 37).

The reaction efficiency can also be defined as the quotient of the sum of the ignition delay and the reaction times divided by the total residence time. The ignition delay and reaction times are set by the flow conditions and species concentrations, along with forward and reverse reaction rates for these eight main reactions (ref. 38):

(1) $H + O_2 \langle = \rangle OH + O$ (5) $H_2 + M \langle = \rangle 2H + M$

(2) $O + H_2 \langle = \rangle OH + H$ (6) $H_2O + M \langle = \rangle H + OH + M$

(3) $OH + H_2 \langle = \rangle H_2O + H$ (7) $OH + M \langle = \rangle H + O + M$

(4) $2OH \langle = \rangle H_2O + O$ (8) $O_2 + M \langle = \rangle 2O + M$

temperature as close as possible to the stagnation temperature. However, note that a decreased entrance Mach number decreases the potential heat addition capacity due to consideration of the Rayleigh criterion (to be discussed in the following section).

The third type of flame phenomenon, the transonic/reverse flow flame, is generated when a temperature rise drives a flow subsonic and locally large combustion pressure rises create adverse flow. Heat addition from combustion tends to decrease local density and increase static pressure, and with an adverse pressure gradient established, the flow velocity is lowered. Coupled with combustion, an increase in flow temperature increases the speed of sound, driving the Mach number toward unity or lower. Thus, locally supersonic flow has the potential to become subsonic without the pressure rise associated with strong shocks. Therefore, it is feasible to have transonic flow with embedded subsonic regions. In addition, adverse pressure gradients generated in the region outside the flame edge can produce regions in which the local static pressure is higher than the stagnation pressure in the combustion region as a result of stagnation pressure losses associated with combustion. At this point, a region of reverse flow can occur. The extent of the reverse flow substantially affects the combustion process by causing increased mixture residence time in the combustor. The potential for the incidence of reverse flow produced by small pressure gradients is important when combustion occurs at low entrance Mach numbers because combustion decreases Mach number. Clearly, the occurrence of subsonic and reverse flow regions in the initially supersonic combustion stream, substantially increases the complexity of the resultant flame structure that must be taken into account.

Supersonic thermal choking.—According to basic gas dynamics theories, any flow can be driven sonic by the addition of heat; in other words, a thermal choke of the supersonic flow occurs if sufficient heat is released by combustion. At low flight Mach numbers, where the ratio of capture flow stagnation enthalpy to stoichiometric combustion enthalpy is low, the heat addition in a scramjet may choke the flow in the combustor. This process is shown in the *T-s* diagram of figure 18. The limit on the heat added to the flow is set by the sonic point of the Rayleigh equation , which is known as the Rayleigh criterion. The following Rayleigh equation (ref. 8, eq. (6.32)) is for a perfect gas flow (the plus is used for subsonic flow while the minus is used for supersonic flow):

$$s = s^* + c_p \ln(T/T^*)$$

$$- R\ln \left\{ 0.5 + 0.5\gamma \pm 0.5[(1+\gamma)^2 - 4\gamma(T/T^*)]^{0.5} \right\}$$

Once the Rayleigh criterion is met, no additional heat (i.e., fuel) can be added in that area without changing upstream flow properties.

Dual-mode combustion.—Since fuel mixing is distributed downstream from the point of injection, the Rayleigh criterion is generally met well into the geometrically diverging portion of the combustor. Further heat addition causes a change in
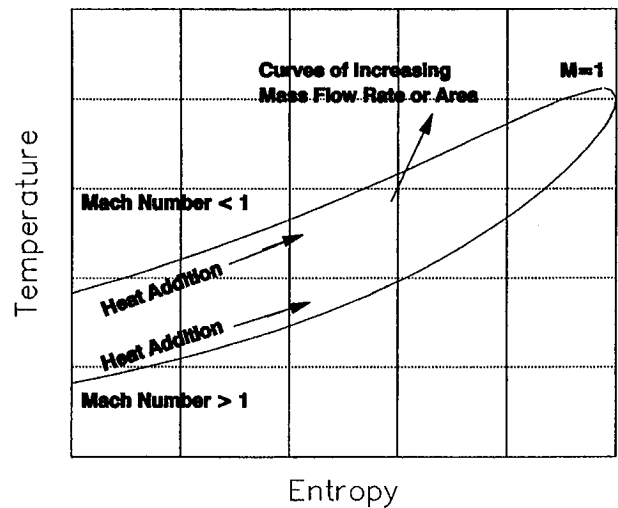

Figure 18.—T-s diagram with Rayleigh curve.

upstream flow conditions, such as the formation of a terminal shock train, which results in a subsonic flow (fig. 19). Because the injection and combustion occur in subsonic flow, this phenomenon is known as dual-mode combustion. As more heat is added, the shock system moves upstream (while in a diverging area) into lower Mach number flow where stagnation pressure losses are reduced.

Subsonic thermal choking.—For a combustor with a nearly constant aerodynamic area (i.e., possibly high separation), the upstream position of the terminal shock system is stabilized so that the Mach number at the exit is sonic. In a combustor with a diverging aerodynamic area, a condition may occur, when heat addition may again drive the flow sonic from a subsonic Mach number. If the combination of heat addition and aerodynamic divergence is correct, the flow may pass through the thermal choke point and become supersonic (fig. 20). If the combination is incorrect, the terminal shock system is moved farther upstream, which moves the choke point farther downstream either to the exit or to a subsonic thermal choke point.
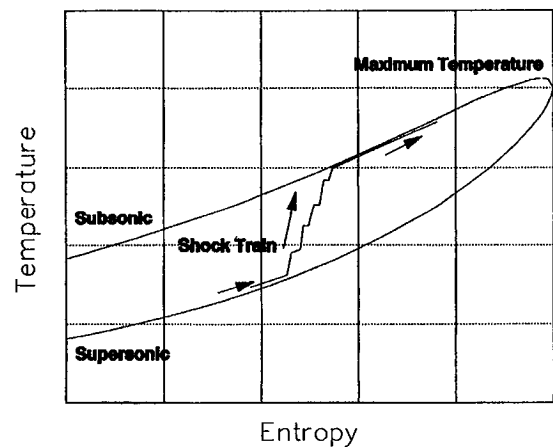

Figure 19.—Rayleigh curve with subsonic thermal choke caused by heat addition with forced upstream shocks.

Unstart.—The terminal shock system can be moved upstream until it is either backed into an aerodynamically convergent section (where it is unstable) or it produces a pressure rise which separates the boundary layer and further aerodynamically contracts the local flow. In either case, the module unstarts. In the low flight Mach number regime, the limit to heat (fuel) addition is the distance upstream the shock system can be moved prior to unstart for the given aerodynamic area and combustion distribution. As just mentioned, the terminal shock train pressure rise separates the boundary layer, and if this separation extends upstream into the inlet, combustor- inlet interaction results. An unchecked cowl boundary layer separation may detach the cowl-lip shock, resulting in increased spillage; thus, for a fixed fuel flow rate, decreased capture drives the shock train farther upstream aggravating the situation. Unstart is typically delayed by (1) staging the fuel injection location downstream in a larger aerodynamic area, (2) increasing the overall aerodynamic expansion area ratio, or (3) increasing the length of the constant-area section (isolator) between the inlet and combustor. Note that these solutions also involve increasing the internal friction drag and overall heat transfer.

Figure 21 illustrates the minimum aerodynamic area that is required for the heat addition from the combustion of stoichiometric hydrogen (ref. 39) without unstart. The data in figure 21 were generated by a real-gas computational cycle analysis program, SRGULL (ref. 40). Ambient temperature hydrogen was used to obtain the data, which are presented in terms of the area ratio relative to the minimum aerodynamic area versus the Mach number at the minimum area. Curves are presented for several combustor entrance stagnation temperatures, which are equal to the flight stagnation temperature (fig. 22) minus any heat transfer. Figure 21 shows that, as Mach number or entrance stagnation enthalpy increases, the required area decreases; in other words, fuel can be staged closer to the minimum area location as the vehicle accelerates.
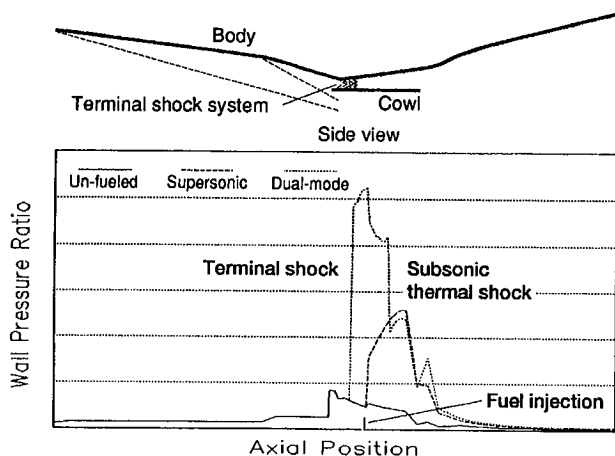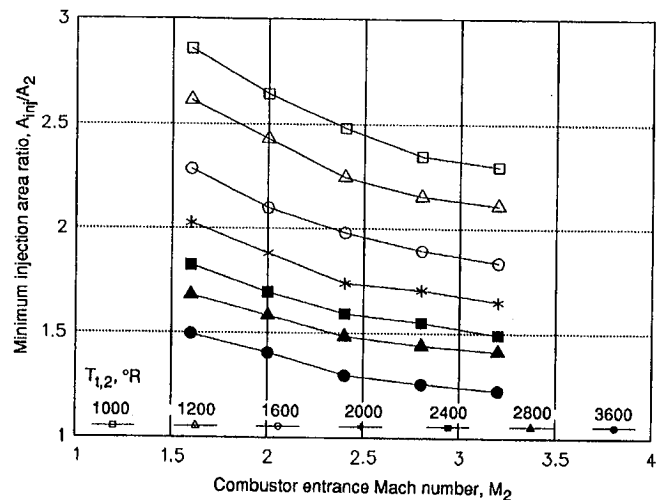
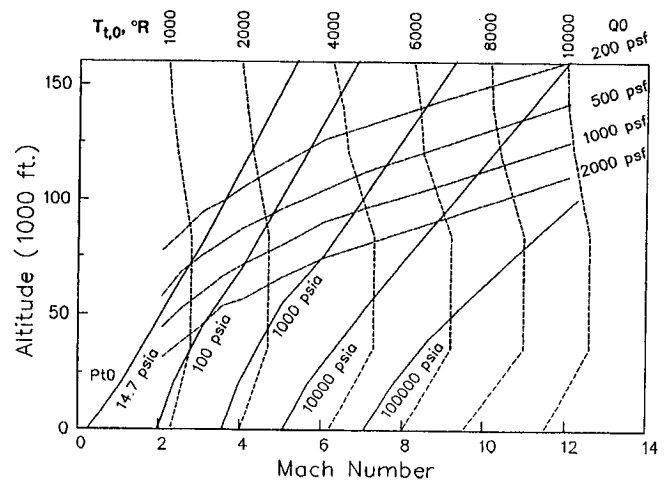Figure 21.—Minimum area required for a heat addition equal to a fuel equivalence ratio of 1.

Figure 22.—Stagnation temperature as a function of flight conditions.

Nozzle

The nozzle of the airframe-integrated scramjet system is generally considered to begin at the location where combustion ends. Usually, the nozzle begins at a station within the module and extends the length of the afterbody. The purpose of the nozzle is to expand the combustor exit flow to free-stream pressure, which must be accomplished with low drag, heat transfer, and stagnation pressure losses (ref. 41). The design of the nozzle, which is mainly the vehicle afterbody, is complicated by the fact that free-stream pressure varies during the mission from sea level static pressure to near vacuum. Therefore, a long nozzle tailored for full expansion to a vacuum and used at a high free-stream pressure could result in flow overexpansion or nozzle flow separation. Concepts, such as baseburning (ref. 42) have been developed to force the nozzle flow along the afterbody and to reduce drag.

Figure 20.—Pressure distribution during thermal choke.

Heat Transfer

Nozzle Boundary Layer

Non-Uniform Flow

Expansion Fan

Spillage Flow

Reacting Gas

Plume (Shear-Mixing Layer)

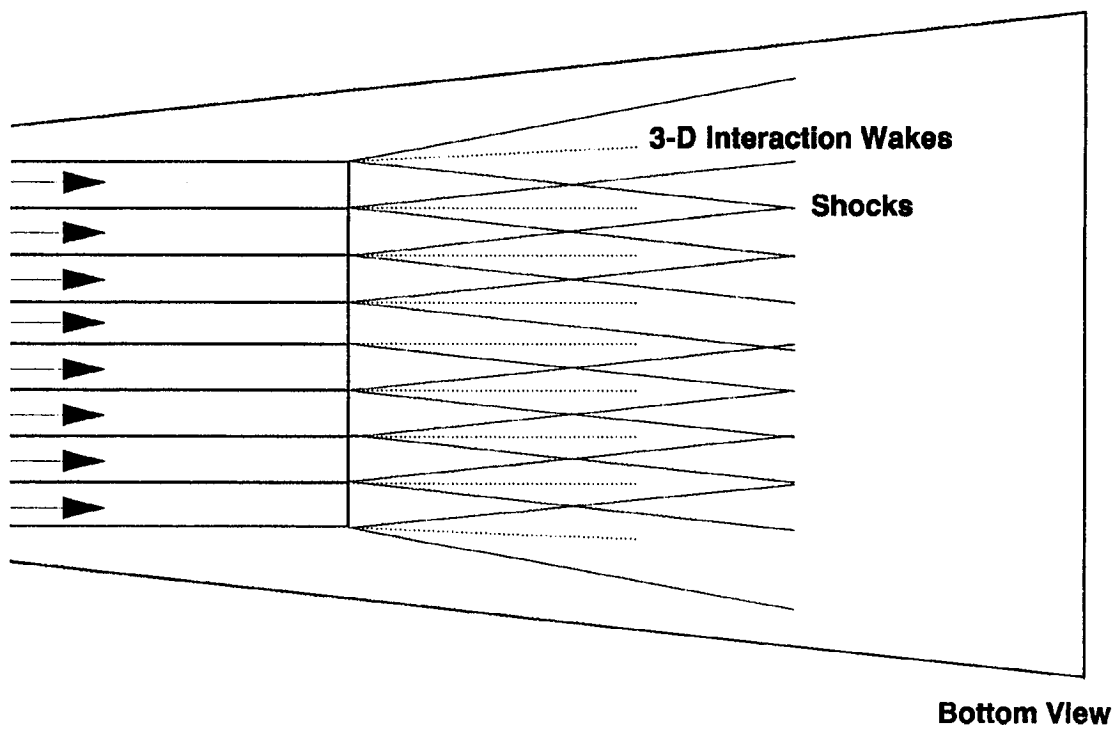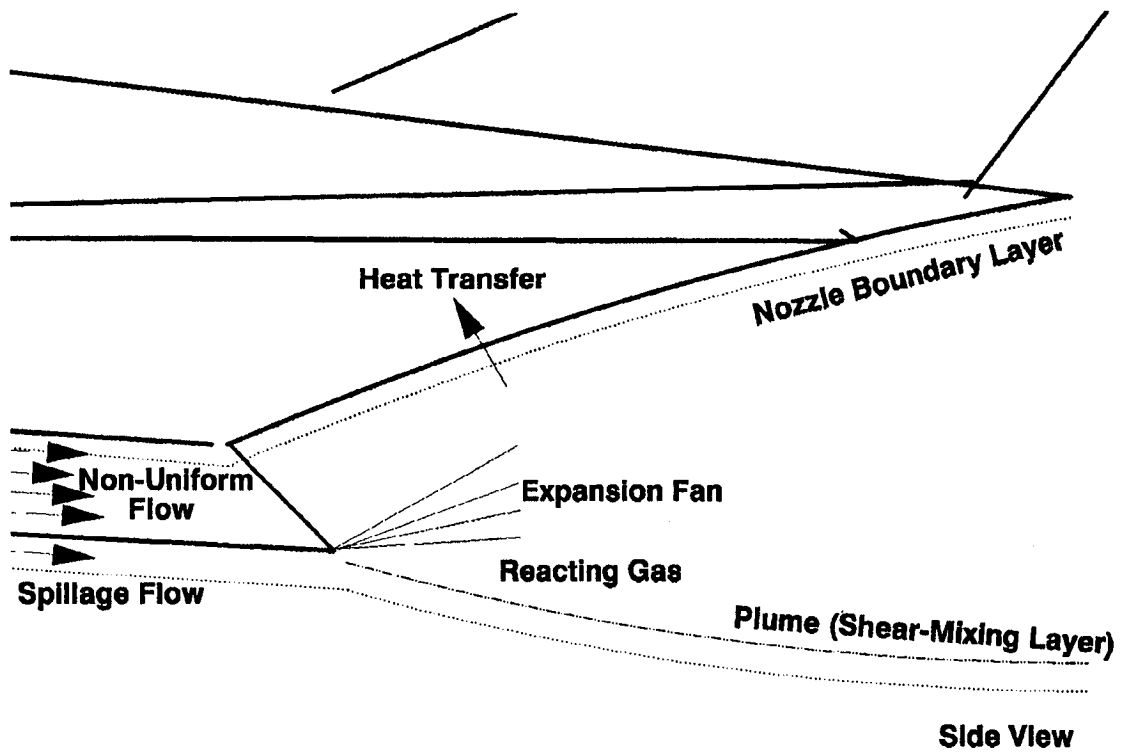**Side View**

3-D Interaction Wakes

Shocks

Bottom View

Figure 23.—Nozzle flow characteristics.

From the perspective of the ideal nozzle expansion process, the combustion pressure is expanded to free-stream pressure to derive the highest flow velocity and to place pressure along the afterbody surface, both of which generate thrust force and moments. Moreover, during the expansion process, it is ideal to recover the vibrational and dissociation energies held by the flow constituents as a result of combustion. If complete recombination occurs during the nozzle residence time, the nozzle exit flow will be in chemical equilibrium and the maximum energy will be released. However, rapid nozzle expansion (which yields low nozzle surface area) produces large pressure and temperature gradients. Therefore, equilibrium flow is unlikely to result, especially if unreacted fuel is present in the combustor exit flow. If the gradients are sufficiently large, the chemical reaction rates can be driven towards zero thus freezing the species concentration.

Nozzle flow is complicated by many factors including nonuniform entrance conditions, viscous effects, internal shocks, adjacent module sidewall wake, and spillage flow (fig. 23). A majority of the flow structures in figure 23 lead to nozzle flow kinetic energy losses which represent stream thrust losses (ref. 43 and 44). Therefore, in nozzle design, the objective is to account for these losses and maximize the kinetic energy efficiency while maintaining a minimum length for weight and heat transfer considerations.

Concluding Remarks

An overview of the airframe-integrated scramjet cycle components and relevant flow features has been presented. The characteristics of each component's aerothermodynamic cycle are given and design tradeoffs are discussed.

Lewis Research Center
National Aeronautics and Space Administration
Cleveland, Ohio, April 8, 1992

References

1. Kepler, L.E.: Mach 5 Test Results of Variable Geometry Scramjet. Proceedings of the Conference on Airbreathing Propulsion for Advanced Missiles and Aircraft, AFAPL–TR–69–52, 1969.
2. King, R.C.: Development and Evaluation of a Mach 7 Hypersonic Scramjet Engine. Proceedings of the Conference on Airbreathing Propulsion for Advanced Missiles and Aircraft, AFAPL–TR–69–52, 1969.
3. Harshman, D.L.: Design and Test of a Mach 7–8 Supersonic Combustion Ramjet Engine. AIAA 3rd Propulsion Joint Specialists Meeting, Washington, D.C., July 1967.
4. Investigation of Low Speed Fixed Geometry Scramjet. AFAPL TR–68–105, General Applied Science Laboratories, Westbury, NY, 1968.
5. Andrews, E.H.; and Mackley, E.A.: Hypersonic Research Engine/ Aerothermodynamic Integration Model. NASA TM X–72824, 1976.
6. Henry, J.R.; and Anderson, G.Y.: Design Considerations for the Airframe-Integrated Scramjet. NASA TM X–2895, 1973.
7. Townend, L.H.; et al.: Forebody Design for the Aerospaceplane. AIAA Paper 90–2472, July 1990.
8. Saad, M.A.: Compressible Fluid Flow, Prentice-Hall, 1985.
9. Dennard, J.S.; and Spencer, P.B.: Ideal-Gas Tables for Oblique-Shock Flow Parameters in Air at Mach numbers from 1.05 to 12.0. NASA TN D–2221, 1964.
10. Lewis, M.J.; Hastings, D.E.: The influence of Flow Non-Uniformities in Air-Breathing Hypersonic Propulsion Systems. AIAA Paper 87–2079, June 1987.
11. Pinckney, S.Z.: Turbulent Heat Transfer Prediction Method for Application to Scramjet Engines. NASA TN D–7810, 1974.
12. Pinckney, Z.P.: Method for Predicting Compressible Turbulent Boundary Layers in Adverse Pressure Gradients. NASA TM X–2302, 1971.
13. Guy, R.W.; et al.: Thermal Design and Analysis of a Hydrogen Burning Wind Tunnel Model of an Airframe-Integrated Scramjet. NASA TM X–73931, 1976.
14. Dash, S.M.: Analysis of Aerospace Vehicle Scramjet Propulsive Fields. NASP CR–1013.
15. Walton, J.: Performance Sensitivity of Hypersonic Vehicles to Changes in Angle of Attack and Dynamic Pressure. AIAA Paper 89–2463, July 1989.
16. Seddon, J.; and Goldsmith, E.L.: Intake Aerodynamics. AIAA, 1985.
17. Andrews, E.H.; Mackley, E.A.; McClinton, C.R.; and Pinckney, S.Z.: The Inlet Starting Problem for a Mach 4 to 8 Scramjet Research Engine. Proceedings of the Conference on Airbreathing Propulsion for Advanced Missiles and Aircraft, AFAPL TR–69–52, 1969.
18. Kantrowitz, A; and Donaldson, C.: Preliminary Investigation of Supersonic Diffusers. NACA WR L–713, 1945.
19. Trexler, C.A.: Inlet Starting Predictions for Sidewall-Compression Scramjet Inlets. AIAA Paper 88–3257, July 1988.
20. Pinckney, S.Z.; Guy, R.W.; and Andrews, E.H., Jr.: Limiting Combustor Pressure Ratio and Combustor-Inlet Interaction Criterion for a Dual-Mode Scramjet Engine (U). NASA TM–86286, 1984.
21. Northam, G.B.; and Anderson, G.Y.: Survey of Supersonic Combustion Ramjet Research at Langley. AIAA Paper 86–0159, July 1986.
22. Kuehn, D.M.: Experimental Investigation of the Pressure Rise Required for the Incipient Separation of Turbulent Boundary Layers in Two-Dimensional Supersonic Flow. NASA Memo 1–21–59A, Feb., 1959.
23. Walton, J.T.; Sagerser, D.A.; Saunders, J.D.; Nguyen, H.L.: Results from M=3.5 Testing of the Modified Government Baseline Engine (U). NASP TP–1003, Jan. 1992.
24. Fernandez, R.; and Rupp, G.: Parametrics from a Small Scale Inlet Test at Mach Inlet Number 3.5 Through 5.5 (U). Presented at the 9th National Aero-Space Plane Symposium, Orlando, FL, Nov. 1–2, 1990.
25. Trexler, C.A.; and Pinckney, S.Z.: Inlet Research for the Langley Airframe Integrated Scramjet. 1983 JANNAF Propulsion Meeting, K.L. Strange, ed., CPIA–Publ–370–Vol–5, Chemical Propulsion Information Agency, Laurel, MD, 1984, pp. 663–670.
26. Guy, R.W.; and Mackley, E.A.: Initial Wind Tunnel Tests at Mach 4 and 7 of a Hydrogen-Burning, Airframe-Integrated Scramjet. AIAA Paper 79–7045, April 1979.
27. Anderson, G.Y.: An Outlook on Hypersonic Flight. AIAA Paper 87–2074, June 1987.
28. Diskin, G.S.; et al.: Mach 2 Combustion Characteristics of Hydrogen-Hydrocarbon Fuel Mixtures. 24th JANNAF Combustion Meeting, Vol. 2, D.L. Becker, ed., CPIA–PUBL–476–Vol–2, Chemical Propulsion Information Agency, Laurel, MD, 1987, pp. 155–169.
29. Ferri, A.: Mixing Controlled Supersonic Combustion. AIAA Paper 72–08, 1972.
30. Orth, R.C.; et al.: Interaction and Penetration of Gaseous Jets in Supersonic Flow. NASA CR–1386, 1969.
31. Orth, R.C.; and Funk, J.A.: An Experimental and Comparative Study of Jet Penetration in Supersonic Flow. AIAA Paper 67–225.

32. Povinelli, L.A.; et al.: Supersonic Jet Penetration Up to Mach 4 into a Mach 2 Air Stream. AIAA Paper 70-92, 1970.
33. Rogers, R.C.: Mixing of Hydrogen Injected from Multiple Injectors Normal to a Supersonic Airstream. NASA TN D-6476, 1971.
34. Jilly, L.F.: HREP-Phase II Combustor Program Final Technical Data Report. AiResearch AP-70-6054, NASA CR-66932, 1970.
35. Huber, P.W.; Schexnayder, C.J., Jr.; and McClinton, C.R.: Criteria for Self-Ignition of Supersonic Hydrogen-Air Mixtures. NASA TP-1457, 1979.
36. Jachimowski, C.J.: An Analytical Study of the Hydrogen Air Reaction Mechanism with Application to Scramjet Combustion. NASA TP-2791, 1988.
37. McClinton, C.R.: Autoignition of Hydrogen Injected Transverse to a Supersonic Airstream. AIAA Paper 79-1239, June 1979.
38. Pergament, H.S.: A Theoretical Analysis of Non-Equilibrium H_2-Air Reactions in Flow Systems. AIAA Paper 79-1239, June 1979.
39. Huff, V.N.; Gordon, S; and Morrell, V.E.: General Method and Thermodynamic Tables for Computation of Equilibrium Composition and Temperature of Chemical Reactions. NACA Report 1037, 1951.
40. Pinckney, S.Z.; and Walton, J.T.: SRGULL: An Advanced Engineering Model for the Prediction of Airframe-Integrated Scramjet Cycle Performance. NASP TM-1120, 1991. (Avail. through COSMIC, University of Athens, Athens, GA, (404) 542-3265, LEW-15093).
41. Stitt, L.E.: Exhaust Nozzles for Propulsion Systems With Emphasis on Supersonic Cruise Aircraft. NASA RP-1235, 1990.
42. Trefny, C.J.: A Computer Program For Estimating the Performance Potential and Fuel Flow Requirements of External Burning for Aerospace Vehicle Transonic Drag Reduction. NASP TM-1034, 1988.
43. Andrews, E.H.; Vick, A.R.; and Craidon, C.B.: Theoretical Boundaries and Internal Characteristics of Exhaust Plumes from Three Different Supersonic Nozzles. NASA TN D-2650, 1965.
44. Stiles, R.J.; and Hoffman, J.D.: Analysis of Steady, Two-Dimensional, Chemically Reacting, Nonequilibrium, Inviscid Flow in Nozzles. AIAA Paper 81-1432, 1981.

Bibliography

History

Waltrup, P.J.: Hypersonic Airbreathing Propulsion: Evolution and Opportunities. Aerodynamics of Hypersonic Lifting Vehicles, AGARD CP-428, AGARD, 1987, Paper 12.

Curran, E. T.; and Stull, F.D.: The Potential Performance of the Supersonic Combustion Ramjet Engine. ASD-TDR-63-336, May 1963.

Ferri, A.: Mixing-Controlled Supersonic Combustion. Annual Review of Fluid Mechanics, Vol. 5, 1973, pp. 301-338.

Waltrup, P.J.: Liquid Fueled Supersonic Combustion Ramjets: A Research Perspective of the Past, Present and Future. AIAA Paper 86-0158, January 1986.

Anderson, G. Y.: An Outlook on Hypersonic Flight. AIAA Paper 87-2074, June 1987.

Townend, L.; et al.: Hypersonic (T-D) "Pinch" and Aerospaceplane Propulsion. AIAA Paper 90-2474, July 1990.

Subscale Testing

Northam, G.B.; and Anderson, G.Y.: Supersonic Combustion Ramjet Research at Langley. AIAA Paper 86-0159, Jan. 1986.

Thomas, S. R.; and Guy, R.W.: Scramjet Testing From Mach 4 to 20: Present Capability and Needs for the Nineties. AIAA Paper 90-1388, June 1990.

Force Accounting

Billig, F.S.; and Sullins, G.A.: A Generalized Method of Force Accounting. NASP CR-1009, Nov. 1987.

Voland, R. T.: Methods for Determining the Internal Thrust of Scramjet Engine Modules from Experimental Data. AIAA Paper 90-2340, July 1990.

Lehrach, R.P.C.: Thrust|Drag Accounting for Aerospace Plane Vehicles. AIAA Paper 87-1966, June 1987.

Computational Fluid Dynamics

White, M.E.; Drummond, J.P.; and Kumar, A.: Evolution and Status of CFD Techniques for Scramjet Applications. AIAA Paper 86-0160, Jan. 1986.

Drummond, J.P.: Supersonic Reacting Internal Flow Fields. NASA TM-103480, 1989.

McClinton, C.R.; Bittner, R.D.; and Kamath, P.S.: CFD Support of NASP Design. AIAA Paper 90-5249, Oct. 1990.

REPORT DOCUMENTATION PAGE

Public reporting burden for this collection of information is estimated to average 1 hour per response, including the time for reviewing instructions, searching existing data sources, gathering and maintaining the data needed, and completing and reviewing the collection of information. Send comments regarding this burden estimate or any other aspect of this collection of information, including suggestions for reducing this burden, to Washington Headquarters Services, Directorate for information Operations and Reports, 1215 Jefferson Davis Highway, Suite 1204, Arlington, VA 22202-4302, and to the Office of Management and Budget, Paperwork Reduction Project (0704-0188), Washington, DC 20503.

1. AGENCY USE ONLY (Leave blank)	2. REPORT DATE	3. REPORT TYPE AND DATES COVERED
	November 1992	Technical Memorandum

4. TITLE AND SUBTITLE

Aerothermodynamic Flow Phenomena of the Airframe-Integrated
Supersonic Combustion Ramjet

5. FUNDING NUMBERS

6. AUTHOR(S)

James T. Walton

7. PERFORMING ORGANIZATION NAME(S) AND ADDRESS(ES)

National Aeronautics and Space Administration
Lewis Research Center
Cleveland, Ohio 44135-3191

8. PERFORMING ORGANIZATION REPORT NUMBER

E-6751

9. SPONSORING/MONITORING AGENCY NAMES(S) AND ADDRESS(ES)

National Aeronautics and Space Administration
Washington, D.C. 20546-0001

10. SPONSORING/MONITORING AGENCY REPORT NUMBER

NASA TM-4376

11. SUPPLEMENTARY NOTES

12a. DISTRIBUTION/AVAILABILITY STATEMENT

Unclassified - Unlimited
Subject Categories 06 and 20

12b. DISTRIBUTION CODE

13. ABSTRACT (Maximum 200 words)

The purpose of this report is to discuss the unique component flow phenomena of the airframe-integrated supersonic combustion ramjet (scramjet) in a format geared towards new players in the arena of hypersonic propulsion. After giving an overview of the scramjet aerothermodynamic cycle, this report then continues to cover individually the characteristics of the vehicle forebody, inlet, combustor, and vehicle afterbody/nozzle. Attention is given to phenomena such as inlet speeding, inlet starting, inlet spillage, fuel injection, thermal choking, and combustor-inlet interaction.

14. SUBJECT TERMS

Scramjet; Supersonic combustion ramjet

15. NUMBER OF PAGES
24

16. PRICE CODE
A03

17. SECURITY CLASSIFICATION OF REPORT	18. SECURITY CLASSIFICATION OF THIS PAGE	19. SECURITY CLASSIFICATION OF ABSTRACT	20. LIMITATION OF ABSTRACT
Unclassified	Unclassified	Unclassified	

National Aeronautics and
Space Administration
Code JTT
Washington, D.C.
20546-0001

NASA

POSTMASTER: If Undeliverable (Section 158
Postal Manual) Do Not Return